

Fatigue Crack Growth Analysis of an Interfacial Crack in Heterogonous Material Using XIGA

Indra Vir Singh and Gagandeep Bhardwaj

Abstract In the present work, the fatigue crack growth analysis of an interfacial cracked plate has been performed by extended isogeometric analysis (XIGA). In isogeometric analysis (IGA), non-uniform rational B-splines (NURBS) are employed for defining the geometry as well as the solution. In XIGA, the merits of isogeometric analysis and extended finite element method are combined together for analyzing the cracked geometries. The crack faces are modeled by discontinuous Heaviside jump function, whereas the singularity in the stress field at the crack tip is modeled by crack-tip enrichment functions. The values of stress intensity factors (SIFs) for the interface cracks are evaluated by XIGA and XFEM. Paris law is employed for computing the fatigue life of an interfacial cracked plate.

1 Introduction

Layered materials/coatings are widely used for protecting the components/structures from corrosion and erosion apart from enhancing the strength and hardness. The structural performance of layered materials depends on the mechanical properties and fracture behavior of the interface. Bilayered materials aim to reduce the residual stresses and avoid debonding at the interface. Therefore, the study of bi-material interfacial cracks becomes important for the design of components and structures. These structures/components have got many challenges due to complexity in accurately evaluating the fracture parameters at the interface. The values of these parameters greatly depend on the internal structure of the material, e.g., the stress intensity factor at the crack tip is affected by the presence of flaws in the vicinity of the crack tip.

I.V. Singh (✉)

Department of Mechanical and Industrial Engineering,
Indian Institute of Technology Roorkee, Roorkee, Uttarakhand, India
e-mail: indrafme@iitr.ac.in

G. Bhardwaj

Mechanical Engineering Department, Thapar University, Patiala, Punjab, India
e-mail: gagandeep.med@thapar.edu

© Springer Nature Singapore Pte Ltd. 2018

P. van Meurs et al. (eds.), *Mathematical Analysis of Continuum Mechanics and Industrial Applications II*, Mathematics for Industry 30,
https://doi.org/10.1007/978-981-10-6283-4_2

Numerical methods are the only choice for an accurate evaluation of the fracture parameters. Over the years, several numerical methods have been developed for evaluating the fracture parameters. Nearly all popular numerical methods discretize a given domain into sub-domains, and then a finite numbers of equations are developed over each domain. The mesh-based methods like FEM, BEM, and FVM can easily and accurately analyze the problems with fixed domain/geometry, but they face a severe challenge in solving the problem involving domain change. To overcome this problem, numerical methods such as element-free Galerkin method [3], boundary node method [14], reproducing kernel particle method [10], cracking particle method [12], and extended finite element method [2] have been developed in past two decades. In these methods, the approximation of geometry introduces some error in the solution as different basis functions are employed for defining the geometry and solution. To cope up with this issue, isogeometric analysis (IGA) has been emerged out as an alternative. In IGA, same basis functions i.e., non-uniform rational B-splines (NURBS) are employed for approximating the geometry as well as the solution. The IGA with partition of unity (PU) enrichment is named as extended isogeometric analysis (XIGA).

2 Isogeometric Analysis

The concept of IGA is introduced by [9] to integrate the computer aided design (CAD) geometry with finite element analysis (FEA). The main aim of IGA is the use of same data set for both design and analysis. In recent times, it gained a lot of attention of the research community due to its accuracy and enhanced capability over standard FEA in analyzing the problems involving complex domains. The NURBS basis functions are employed to approximate the geometry and solution in the physical space. Its name (“isogeometric”) is due to fact that the use of NURBS leads to an exact geometric description of the domain, whereas in standard finite element analysis, it is necessary to approximate the geometry by finite elements. The geometry in IGA is modeled accurately even at the coarse mesh, which is difficult to achieve by standard Lagrange basis function in FEA. The details of the B-spline, knot vector, basis function, and NURBS are provided below.

2.1 B-Splines

B-splines are built from piecewise polynomial functions i.e., from a set of polynomial functions. B-spline consists of n -polynomial basis functions of order p .

2.2 Knot Vectors

Knot vectors are used to define the piecewise polynomial basis functions. A knot vector (Ξ) is defined by a set of coordinates in the parametric space $\xi \in [0, 1]$, which provides the information about the subinterval i.e., element. A knot vector (Ξ) in one dimension is defined by a nondecreasing set of coordinates in the parametric space as [4, 7, 13].

$$\Xi = \{\xi_1, \xi_2, \dots, \xi_{n+p+1}\}, \text{ with } \xi_i \in R \text{ and } \xi_i \leq \xi_{i+1} \quad (1)$$

where, ξ_i and n represent a knot and number of univariate spline basis functions defined on the knot vector, respectively, and i is the knot index whose value varies from $i = 1, 2, 3, \dots, n + p + 1$.

2.3 B-Spline Basis Functions

The B-spline functions are defined recursively starting with the piecewise constants ($p = 0$)

$$N_{i,0}(\xi) = \begin{cases} 1 & \xi_i \leq \xi \leq \xi_{i+1} \\ 0 & \text{otherwise} \end{cases} \quad \text{for } p = 0 \quad (2a)$$

$$N_{i,p}(\xi) = \frac{\xi - \xi_i}{\xi_{i+p} - \xi_i} N_{i,p-1}(\xi) + \frac{\xi_{i+p+1} - \xi}{\xi_{i+p+1} - \xi_{i+1}} N_{i+1,p-1}(\xi) \quad \text{for } p \geq 1 \quad (2b)$$

2.4 Non-uniform Rational B-Splines

Non-uniform rational B-splines (NURBS) are piecewise rational polynomials constructed from B-splines. The term nonuniform refers to the use of nonuniform knot vectors. In general, the NURBS are defined as,

$$R_{i,p}(\xi) = \frac{w_i N_{i,p}(\xi)}{W(\xi)} = \frac{w_i N_{i,p}(\xi)}{\sum_{i=0}^n w_i N_{i,p}(\xi)} \quad (3)$$

where, $R_{i,p}(\xi)$ defines NURBS, w_i refers to weights associated with the i th control point, and $N_{i,p}(\xi)$ defines B-spline basis functions of order p .

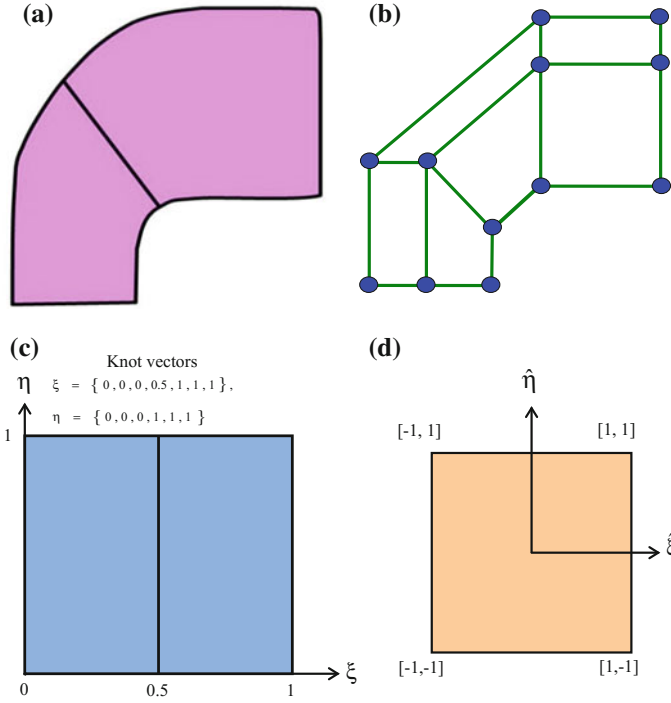


Fig. 1 **a** Physical space. **b** Control mesh. **c** Parametric space. **d** Parent element

2.5 Spaces and Mappings

In isogeometric analysis, different spaces are employed. These spaces are physical space, control mesh, parameter space, index space, and parent element. In physical space, the actual geometry is represented by a linear combination of the basis functions and the control points. The basis functions do not interpolate the control points except at the end. The physical mesh can be divided into elements by knot spans. The physical space is represented in Fig. 1a. The control mesh (control net) is defined by the control points. The control mesh interpolates all control points. It controls the geometry but does not coincide with the physical mesh. The control variables are the degrees of freedom and are located at the control points. A typical control mesh is shown in Fig. 1b. The parametric space is formed by the knot spans. The elements are defined in this space as nonzero knot spans $[\xi_i, \xi_{i+1}] \times [\eta_j, \eta_{j+1}]$. The NURBS basis functions $R_{i,j}^{p,q}(\xi, \eta)$ are defined over the parametric space. Each element in the physical space depicts the image of the corresponding element in the parametric space. The parametric space for a particular knot vector is shown in Fig. 1c.

The parent element describes a constant space $[-1, 1] \times [-1, 1]$ where the integration is performed for each element. The parameters ξ and η of the parametric

space are mapped onto the $\hat{\xi}$ and $\hat{\eta}$ in the parent element so that the Gauss quadrature can be used for integration. A typical parent element is shown in Fig. 1d.

In IGA, two transformations are performed from physical space to the parent element for the generation of Gauss points. First, the physical space is transformed into parametric space, which is constructed from the knot spans. The parametric space is then transformed into parent element.

3 Extended Isogeometric Analysis

The NURBS basis functions are suitable for the problems requiring smooth solutions due to their higher order continuity. However, for modeling the problems involving defects (crack, holes and inclusions), IGA approximation enriched using partition of unity (PU) is known as extended isogeometric analysis (XIGA). PU enrichment is quite effective and efficient method for analyzing static and moving discontinuities in the structures, whereas IGA is quite accurate and efficient in analyzing complex geometries [15]; hence, the merits of both XFEM (PU enrichment) and IGA are exploited in XIGA for the accurate modeling of the components/structures. The isogeometric formulation for the analysis of structure/component is explained in [5, 6].

3.1 XIGA Approximation for Cracks

At a particular control point corresponding to ξ_i in the parametric space, the displacement approximation for cracks can be written in a generalized form as,

$$\mathbf{u}^h(\xi) = \sum_{i=1}^{n_{en}} R_i(\xi) \mathbf{u}_i + \left\{ \sum_{j=1}^{n_{cf}} R_j(\xi) [H(\xi) - H(\xi_i)] \mathbf{a}_j \right\} B_H + \left[\sum_{k=1}^{n_{ct}} R_k(\xi) \left\{ \sum_{\alpha=1}^4 [\beta_\alpha(\xi) - \beta_\alpha(\xi_i)] \mathbf{b}_k^\alpha \right\} \right] B_T \quad (4)$$

where, \mathbf{u}_i = parameters associated with a particular control point, n_{en} = number of basis functions per element defined as $n_{en} = (p + 1) \times (q + 1)$, n_{cf} = number of basis functions whose support is completely intersected by the crack face, n_{ct} = number of basis functions whose support is partially intersected by the crack tip, \mathbf{a}_j = additional control point enriched degrees of freedom associated with Heaviside function $H(\xi)$, \mathbf{b}_k^α = additional control point enriched degrees of freedom associated with asymptotic crack tip enrichment functions, β_α , B_H = blending function for the Heaviside function, B_T = blending function for the crack tip, $H(\xi)$ = Heaviside function, β_α = crack-tip enrichment functions.

At a particular Gauss point in an element, if the parametric coordinate ξ corresponding to that particular Gauss point is above the crack face, then $H(\xi)$ is equal to +1 and if ξ lies below the crack face, then $H(\xi)$ is -1. Similarly, discontinuous Heaviside function $H(\xi_i)$ takes value +1 and -1 if a control point lies above and below the crack face respectively.

3.2 XIGA Formulation

As mentioned above, Eq.(4) defines the enriched displacement approximation at a particular point in XIGA. The first term on right-hand side of Eq.(4) represents the standard finite element approximation, while the remaining enrichment terms are used to model crack. Using the approximation defined in Eq.(4), the elemental matrices \mathbf{k} and \mathbf{f} are defined as,

$$\mathbf{k}_{ij}^e = \begin{bmatrix} \mathbf{k}_{ij}^{uu} & \mathbf{k}_{ij}^{ua} & \mathbf{k}_{ij}^{ub} \\ \mathbf{k}_{ij}^{au} & \mathbf{k}_{ij}^{aa} & \mathbf{k}_{ij}^{ab} \\ \mathbf{k}_{ij}^{bu} & \mathbf{k}_{ij}^{ba} & \mathbf{k}_{ij}^{bb} \end{bmatrix} \quad \text{and} \quad \mathbf{f}_i^e = \{ \mathbf{f}_i^u \quad \mathbf{f}_i^a \quad \mathbf{f}_i^{b1} \quad \mathbf{f}_i^{b2} \quad \mathbf{f}_i^{b3} \quad \mathbf{f}_i^{b4} \}^T \quad (5)$$

where,

$$\mathbf{k}_{ij}^{rs} = \int_{\Omega^e} (\mathbf{B}_i^r)^T \mathbf{C} \mathbf{B}_j^s d\Omega, \quad \mathbf{f}_i^u = \int_{\Omega^e} \mathbf{R}_i^T \mathbf{b} d\Omega + \int_{\Gamma_t} \mathbf{R}_i^T \hat{\mathbf{t}} d\Gamma \quad (6)$$

$$\mathbf{f}_i^a = \int_{\Omega^e} \mathbf{R}_i^T H \mathbf{b} d\Omega + \int_{\Gamma_t} \mathbf{R}_i^T H \hat{\mathbf{t}} d\Gamma, \quad \mathbf{f}_i^{b\alpha} = \int_{\Omega^e} \mathbf{R}_i^T \beta_\alpha \mathbf{b} d\Omega + \int_{\Gamma_t} \mathbf{R}_i^T \beta_\alpha \hat{\mathbf{t}} d\Gamma \quad (7)$$

where, R_i represents the NURBS basis function, and \mathbf{B}_i^u , \mathbf{B}_i^a , \mathbf{B}_i^b , $\mathbf{B}_i^{b\alpha}$, \mathbf{B}_i^c , and \mathbf{B}_i^d are the matrices of derivatives of NURBS basis function.

$$\mathbf{B}_i^u = \begin{bmatrix} R_{i,X_1} & 0 \\ 0 & R_{i,X_2} \\ R_{i,X_2} & R_{i,X_1} \end{bmatrix} \quad \mathbf{B}_i^a = \begin{bmatrix} (R_i)_{,X_1} H & 0 \\ 0 & (R_i)_{,X_2} H \\ (R_i)_{,X_2} H & (R_i)_{,X_1} H \end{bmatrix} \quad \mathbf{B}_i^b = \begin{bmatrix} \mathbf{B}_i^{b1} & \mathbf{B}_i^{b2} & \mathbf{B}_i^{b3} & \mathbf{B}_i^{b4} \end{bmatrix}$$

For the details on the selection of enriched control points, integration in discontinuous elements, computation of stress intensity factors, fatigue crack growth criterion, and Paris law, please refer [6].

In the present work, maximum hoop (circumferential) stress criterion [8] is used for crack growth direction.

$$\theta_c = 2 \tan^{-1} \left(\frac{K_I - \sqrt{K_I^2 + 8K_{II}^2}}{4K_{II}} \right) \quad (8)$$

4 Fatigue Crack Growth in Bi-material

The fatigue crack growth analysis of an interfacial edge crack or center crack in bi-material has been performed by both XIGA and XFEM under plane stress condition. The domain containing an edge or center crack is subjected to tensile load of $\sigma_{\min} = 0$ MPa and $\sigma_{\max} = 70$ MPa at the top edge, whereas the bottom edge is constrained in y -direction. Each material comprising the bi-material is assumed to be homogenous and isotropic. The upper half of the domain consists of low stiffness material (material-1 or $m1$), whereas the lower half consists of a high stiffness material (material-2 or $m2$). The material properties of Material-1 ($m1$) and Material-2 ($m2$) are given in Table 1. The numerical simulations are performed using a control net of 30×60 in case of XIGA and a mesh size of 50×100 in case of XFEM.

4.1 Edge Crack Growth

A bi-material rectangular domain of dimension $50 \text{ mm} \times 100 \text{ mm}$ with an interfacial edge crack of initial length, $a = 5 \text{ mm}$, is taken for the fatigue crack growth analysis as shown in Fig. 2.

The normal stress (σ_{yy}) contour plot for a crack length of 5.0 mm is shown in Fig. 3. The variation of equivalent SIF with crack extension is shown in Fig. 4. The crack growth direction is obtained from Eq. (8), and then the crack is extended by 2 mm in that direction. The problem is again solved for new crack length, and SIFs values and crack growth direction are obtained again. This process continues till the final failure i.e., simulation stops when $K_{Ieq} \geq \min \{(K_{IC})_{m1}, (K_{IC})_{m2}\}$. The fatigue life of bi-material cracked domain evaluated by XIGA using Paris law is presented in Fig. 5. The failure life and crack length (at the time of failure) are found to be 3.1×10^6 cycles and 14 mm , respectively.

Table 1 Material properties of aluminum alloy ($m1$) [1] and steel ($m2$) [11]

Property	Aluminum (m1)	Steel (m2)
Elastic modulus (GPa)	70	200
Poisson's ratio	0.33	0.30
Fracture toughness (MPa $\sqrt{\text{mm}}$)	917.06	1897.36
Paris law constant $m/\text{cycle (MPa}\sqrt{\text{m}})^{-M}$	1×10^{-12}	2.087136×10^{-12}
Paris law exponent	3	3

Fig. 2 Interfacial edge cracked bi-material body with loading and boundary conditions

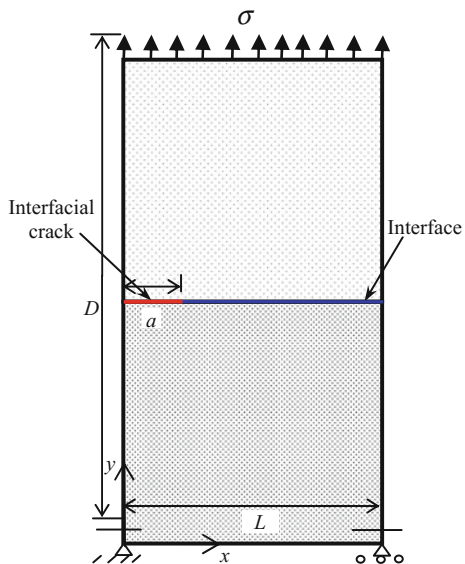


Fig. 3 Contour plot of σ_{yy} (MPa) for an interfacial edge crack in bi-material

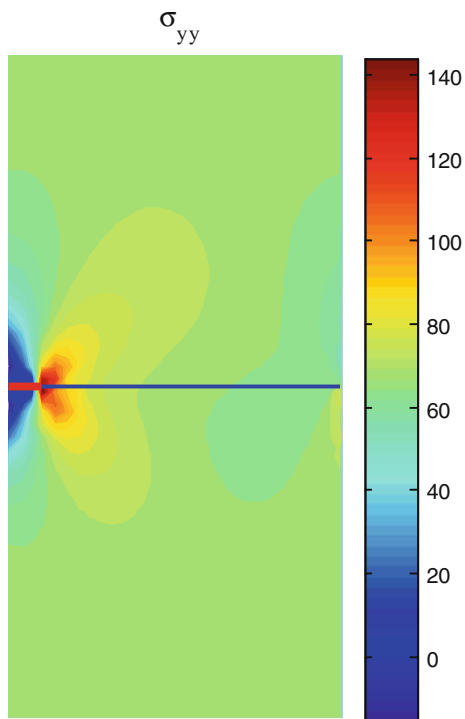


Fig. 4 K_{Ieq} variation with crack extension for an interfacial edge crack in bi-material

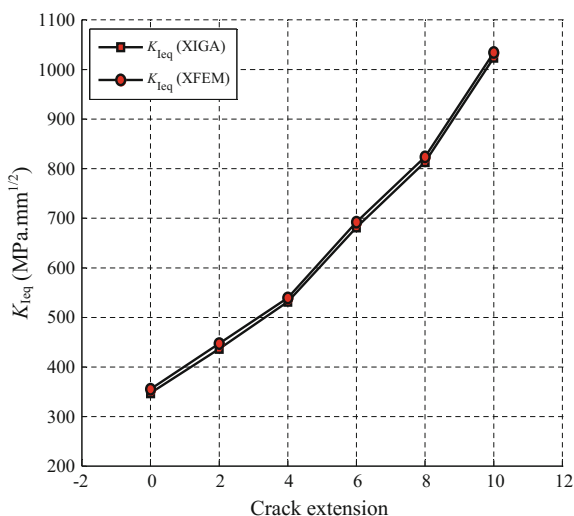
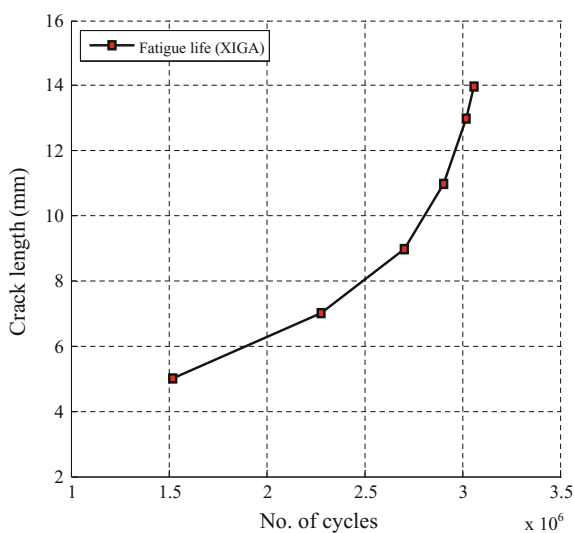


Fig. 5 Fatigue life variation with crack length for an interfacial edge crack in bi-material



4.2 Center Crack Growth

A bi-material rectangular domain of size $50\text{ mm} \times 100\text{ mm}$ with an interfacial center crack of length, $2a = 10\text{ mm}$, is taken for analysis as shown in Fig. 6. The contour plot of normal stress (σ_{yy}) for a crack length of 10 mm is shown in Fig. 7. The variation of equivalent SIF (K_{Ieq}) with crack length is shown in Fig. 8. The crack

Fig. 6 Interfacial center cracked bi-material body with loading and boundary conditions

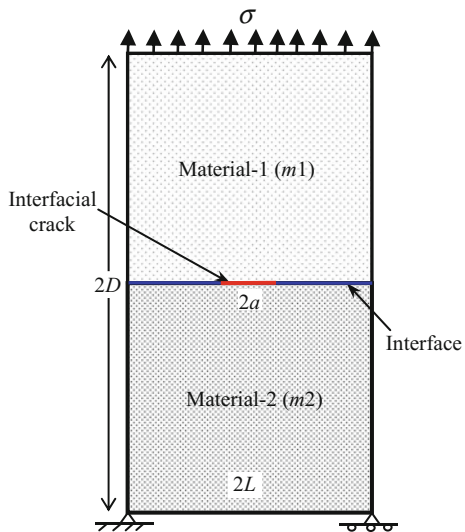


Fig. 7 Contour plot of σ_{yy} (MPa) for an interfacial center crack in bi-material

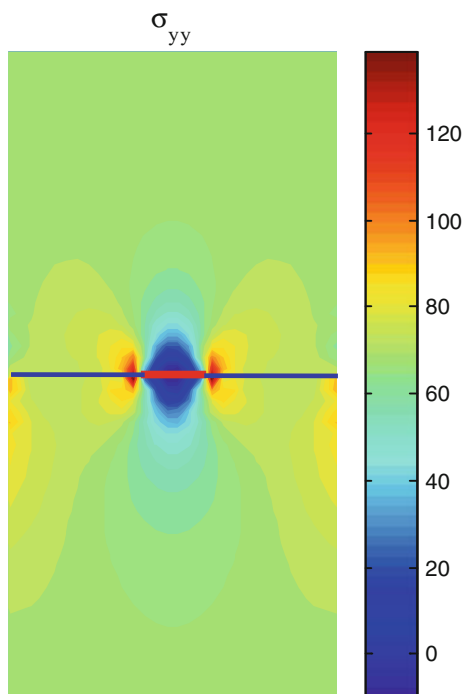


Fig. 8 K_{Ieq} variation with crack extension for an interfacial center crack in bi-material

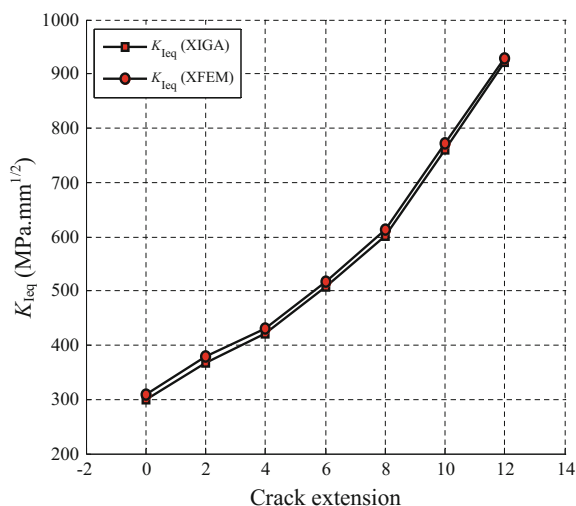
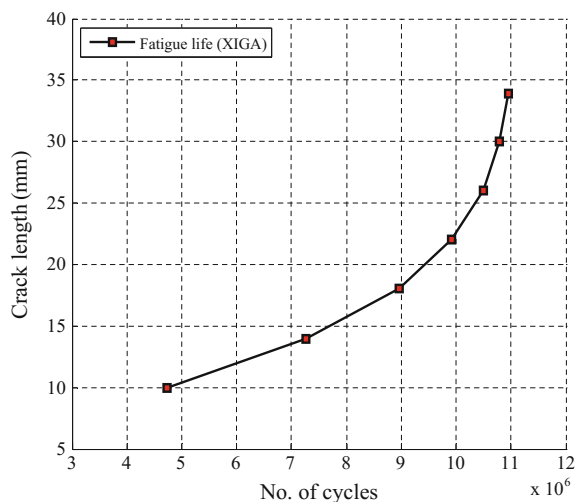


Fig. 9 Fatigue life variation with crack length for an interfacial center crack in bi-material



growth direction is obtained from Eq. (8), and then crack is extended by 2 mm in that direction. The problem is again solved for new crack length, and SIFs values and crack growth direction are obtained again. This process continues till the final failure i.e., simulation stops when $K_{Ieq} \geq \min \{(K_{IC})_{m1}, (K_{IC})_{m2}\}$.

The fatigue life of bi-material cracked body evaluated by XIGA using Paris law is shown in Fig. 9. The failure life and corresponding crack length at the time of failure are found to be 1.1×10^7 cycles and 33.9 mm.

5 Conclusions

In this work, the IGA is extended to solve interfacial fracture mechanics problems. The fatigue crack growth analysis of edge or center crack in bi-material domain is performed under mode-I loading. The mode-I SIF values obtained by XIGA (using a control net of 30×60) are compared with the XFEM using a mesh size of 50×100 . In bi-material, the crack kinks out from the interface and travels in material with lower fracture toughness along the interface. These simulations show that the results obtained by XIGA using coarse control net are in good agreement with those obtained by XFEM using fine mesh.

References

1. Arola, D., Huang, M.P., Sultan, M.B.: The failure of amalgam dental restorations due to cyclic fatigue crack growth. *J. Mater. Sci.: Mater. Med.* **10**, 319–327 (1999)
2. Belytschko, T., Black, T.: Elastic crack growth in finite elements with minimal remeshing. *Int. J. Numer. Methods Eng.* **45**, 601–620 (1999)
3. Belytschko, T., Gu, L., Lu, Y.Y.: Fracture and crack growth by element free Galerkin methods. *Model. Simul. Mater. Sci. Eng.* **2**, 519–534 (1994)
4. Bhardwaj, G., Singh, I.V., Mishra, B.K.: Stochastic fatigue crack growth simulations of interfacial crack in bi-layered FGM's using XIGA. *Comput. Methods Appl. Mech. Eng.* **284**, 186–229 (2015)
5. Bhardwaj, G., Singh, I.V., Mishra, B.K.: Numerical simulation of functionally graded cracked plates using NURBS based XIGA under different loads and boundary conditions. *Compos. Struct.* **126**, 347–359 (2015)
6. Bhardwaj, G., Singh, S.K., Singh, I.V., Mishra, B.K., Rabczuk, T.: Fatigue crack growth analysis of an interfacial crack in heterogeneous materials using homogenized XIGA. *Theor. Appl. Fract. Mech.* **85**, 294–319 (2016)
7. Cottrell, J.A., Hughes, T.J.R., Reali, A.: Studies of refinement and continuity in isogeometric structural analysis. *Comput. Methods Appl. Mech. Eng.* **196**, 4160–4183 (2007)
8. Erdogan, F., Sih, G.C.: On the crack extension in plates under plane loading and transverse shear. *ASME J. Fluids Eng.* **85**, 519–525 (1963)
9. Hughes, T.J.R., Cottrell, J.A., Bazilevs, Y.: Isogeometric analysis: CAD, finite elements, NURBS, exact geometry and mesh refinement. *Comput. Methods Appl. Mech. Eng.* **194**, 4135–4195 (2005)
10. Liu, W.K., Jun, S., Zhang, Y.F.: Reproducing kernel particle methods. *Int. J. Numer. Methods Eng.* **20**, 1081–1106 (1995)
11. Pathak, H., Singh, A., Singh, I.V.: Fatigue crack growth simulations of bi-material interfacial cracks under thermo elastic loading by extended finite element method. *Eur. J. Comput. Mech.* **22**, 79–104 (2013)
12. Rabczuk, T., Belytschko, T.: Cracking particles: a simplified meshfree method for arbitrary evolving cracks. *Int. J. Numer. Methods Eng.* **61**, 2316–2343 (2004)
13. Singh, I.V., Bhardwaj, G., Mishra, B.K.: A new criterion for modeling multiple discontinuities passing through an element using XIGA. *J. Mech. Sci. Technol.* **29**, 1131–1143 (2015)
14. Yan, A.M., Nguyen-Dang, H.: Multiple-cracked fatigue crack growth by BEM. *Comput. Mech.* **16**, 273–280 (1995)
15. Wall, W.A., Frenzel, M.A., Cyron, C.: Isogeometric structural shape optimization. *Comput. Methods Appl. Mech. Eng.* **197**, 2976–2988 (2008)

Mathematical Analysis of Continuum Mechanics and
Industrial Applications II

Proceedings of the International Conference CoMFoS16

van Meurs, P.; Kimura, M.; Notsu, H. (Eds.)

2018, VIII, 193 p. 44 illus., 25 illus. in color., Hardcover

ISBN: 978-981-10-6282-7